Bulletin Géodésique (1995) 69:252–260

Bulletin Géodésique

Gravity anomalies from satellite altimetry: comparison between computation via geoid heights and via deflections of the vertical

A. Olgiati [1], G. Balmino [1], M. Sarrailh [1], and C. M. Green [2]

[1] Bureau Gravimétrique International, CNES/GRGS, 18 Av. Edouard Belin, F-31055 Toulouse Cedex, France
[2] GETECH, Department of Earth Sciences, University of Leeds, Leeds, LS2 9JT, United Kingdom

Received 10 June 1994; Accepted 27 February 1995

Abstract

The accumulation of good quality satellite altimetry missions allows us to have a precise geoid with fair resolution and to compute free air gravity anomalies easily by fast Fourier transform (FFT) techniques.

In this study we are comparing two methods to get gravity anomalies. The first one is to establish a geoid grid and transform it into anomalies using inverse Stokes formula in the spectral domain via FFT. The second one computes deflection of the vertical grids and transforms them into anomalies.

The comparison is made using different data sets: Geosat, ERS-1 and Topex-Poseidon exact repeat misions (ERMs) north of 30°S and Geosat geodetic mission (GM) south of 30°S. The second method which transforms the geoid gradients converted into deflection of the vertical values is much better and the results have been favourably evaluated by comparison with marine gravity data.

Introduction

Computing free air gravity anomalies (FAA) from satellite altimetry has become an important technique in marine geodesy and geophysics. Early results were obtained more than ten years ago from Geos3 and Seasat by Haxby et al. (1983) and since then refined by many groups. It has often been done by converting geoid height grids into FAA grids (Knudsen et al., 1992). Another way to do it, which is getting more and more frequently used, is to convert geoid gradient derived deflection of the vertical grids into FAA grids (Sandwell, 1992).

This paper presents a comparison between these two methods with a special emphasis on practical aspects and problems encountered during the gridding of geoid heights, the gridding of north and east deflections of the vertical and finally the FFT techniques used for conversion into FAA; we restricted our investigation to the FFT techniques and did not use least squares collocation, although thought to be a good method for our type of problem (Rapp and Basic, 1992), for it is generally more demanding in computer time.

The first method is based on the direct gridding of the geoid heights measured along the sub-satellite tracks (either from individual tracks or from averaged stacked arcs). This gridding is made after a cross-over adjustment to remove most of the orbit error and after a «spline adjustment» to avoid artefacts near bad cross-overs. A one year stacked arc of Topex-Poseidon was first adjusted over the whole globe and formed the basis for subsequent adjustments. The FAA are then derived by Fourier transform, taking care of some correction to the approximation of Stokes function, trying to reduce the errors due to flat Earth approximation and truncation of the integral, using a Wiener filter to take into account the data noise and using a remove-restore technique based on a 360 degree-order spherical harmonic reference model.

The second method does not require a preliminary cross-over adjustment. It derives the geoid gradients along each altimetric profile, after ad'hoc smoothing, and interpolates cross-track gradients from cross-over bi-directional information. The north and east deflection of the vertical components are thus computed at each data point and gridded. These two deflection grids are finally converted into FAA via FFT, with similar precautions as for the first method.

The comparison is first made with ERM non-dense data, and then with GM data where the cross-track distance is smaller than the along-track resolution. In both cases, the comparison is also made with marine gravity data and with the global FAA grid computed by Sandwell & Smith (1992).

Correspondence to: G. Balmino

I- METHODOLOGY

I.1- From geoid to anomalies

First step: data stacking

To get the geoid, we need to subtract the sea surface dynamic topography (SSDT) from the mean sea surface (MSS). To get the MSS, we first need to stack the different cycles of an ERM together. This is easy to do for Topex-Poseidon data thanks to the quality of the orbit: we can directly compute mean values of height and position with the values of the different cycles for each point of a track; to insure the quality of the stacked profile, a mean value *(derived by weighting data as a function of their distance to the reference point)* is computed only if we have at least 24 values out of 37 cycles. For Geosat and ERS-1, the orbit error is greater than the oceanic variability and we need to adjust the different cycles together prior to averaging the different height values. Not doing that would produce some jumps in the stacked profile when one of the cycles has no data. Besides and in order to minimize the effect of geoid gradients, the mean value is computed by using residual quantities with respect to the OSU91A model (Rapp et al., 1991).

Each satellite data set is thus stacked over a one year period, which is enough to remove most of the oceanic variability.

Second step: orbit error reduction

Once we have the different stacked data sets, we operate a cross-over adjustment to remove most of the non geographically correlated part of the orbit error (Balmino, 1992). Our cross-over orbit error adjustment software is composed of two steps: the cross-over search and the adjustment.

Cross-over search: the cross-overs can be searched between the arcs of 1, 2 or 3 satellites. Each data set is cut into ascending and descending arcs which will be adjusted separately. The Equator crossing longitude is computed for each arc, as well as other parameters which allow us to have a theoretical track based on satellite dynamics formulas. For each pair of arcs suspected to intersect, a theoretical cross-over position is quickly computed. Then a dichotomous search locates on each arc the exact position of the cross-over and both cross-over heights are interpolated (linearly, with splines or with smoothing splines). This first step takes 10 CPU-hours on a Sun SPARC station IPX or 12 CPU-minutes on a CDC Cyber 2000 for 100.000 cross-overs in the case of sparse data, or for 200.000 cross-overs for dense data.

Adjustment: each arc is adjusted assuming an orbit error function such as: orthogonal polynomials with 1, 2 or 3 unknowns (bias + tilt + curvature) or sinusoidal functions with up to 5 unknowns (terms at one or two cycles per revolution). The sinusoidal functions are used only for large areas. Two software systems have been written to perform these adjustments: a direct algorithm with inversion of the least squares matrix and an iterative algorithm.

When working with three satellites at a time such as Geosat, ERS-1 and Topex-Poseidon, we first do an adjustment of Topex-Poseidon alone because its orbit error is much smaller than for the others. Any adjustment of this type requires some constraints to be added to the system of equations, to insure the stability of the adjustment. We adopted the simple method by which, for each unknown u, we add an a priori value equation u=0. Such an equation would have an undesirable effect if it was not weighted with a very low weight with respect to the observation equations. In practice it proves to be adequate to stabilize the system with, as shown by several tests using the two above-mentioned algorithms, no effect on the good relative adjustment between the arcs. The constraints may impact the reference frame in which the adjusted sea surface heights are obtained, but almost not the gravity anomalies to be derived from them because of their long wavelength nature. An interactive graphic software system then allows us to see not only the geographical distribution of the cross-over height differences before and after adjustment, but also the corrections that are applied on ascending or descending arcs to check that the adjustment is satisfactory not only in the root mean square (RMS) sense.

Once this best satellite data set is adjusted, we decide that it serves as an absolute reference for the other satellites and we do a three satellite adjustment with fixed Topex-Poseidon arcs; in other words, we adjust Geosat and ERS-1 on Topex-Poseidon. When we do this, we still take into account Geosat/ERS-1 cross-overs. Each cross-over is considered with a weight depending on the precisions assumed on the crossing satellite altimeters, and also with another weight depending on the number of cross-overs of each family of arcs, so as not to privilege denser data sets like ERS-1 (35-day orbit against 11-day orbit for Topex-Poseidon).

Third step: spline adjustment

After having done the orbit error adjustment, there are still height differences at cross-overs. These differences are due, among other causes, to:

- altimeter noise
- bad measurements that may not have been eliminated
- poor corrections applied to the measurements, especially the tidal correction near coasts
- residual orbit error, which is supposed to be very small (something not well absorbed by the orbit error model chosen)
- residual oceanic circulation signal, especially in places where all the cycles covering the one year period where not present; also signals with 2 year or 3 year cycles.

Whereas the relative accuracy on each arc may be quite good, these residual errors at cross-overs may force us to

over-smooth in gridding, independently of the algorithm. Otherwise, it might result in artefacts such as on figure 1. The effect is even more disastrous when recovering the gravity anomalies.

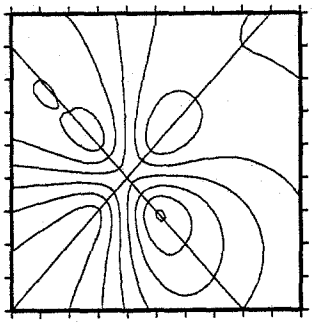

Figure 1. Artefacts in a geoid grid due to a bad cross-over

A pragmatic approach since the error may be on arc A, on arc B or on both arcs (fig. 2) is to assume that the MSS is somewhere between arc A and arc B. The idea is then to add a spline function to each arc so that they cross exactly at the same height. Thus the error relative to the MSS will not be worse than it would be without modifying the arcs, and we get rid of the artefact. This is what we have called «spline adjustment».

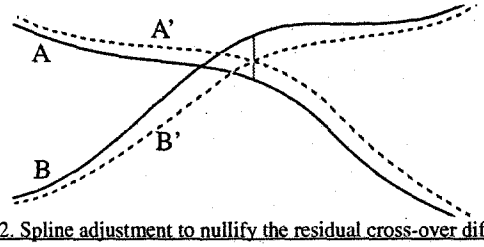

Figure 2. Spline adjustment to nullify the residual cross-over differences

In practice, we consider an arc A with all its cross-overs with arcs of the same or of different satellites. The heights at the cross-overs are computed with smoothing splines so as to take into account the noise of the altimeter. Let $\Delta h(i)$ be the height difference at cross-over number i, satA be the satellite of arc A and satB the satellite of crossing arc B; then we compute a spline function for arc A which will take the following value at cross-over i:

$$\Delta h\,(i) \times \frac{\text{precision (satA)}}{\text{precision (satA)} + \text{precision (satB)}}$$

and a similar formula for arc B, the precision being estimated for each satellite, for example by the RMS of the cross-over height differences for this satellite after adjustment.

For instance, two arcs of a common satellite will be moved by half the difference at the cross-over. The spline functions of Akima (1970) are used to avoid oscillations when two cross-overs are very close.

After this adjustment, the RMS at cross-overs are nullified, and the artefacts seen previously disappear (or are reduced in places where three arcs have three very close bad cross-overs).

Fourth step: from MSS to residual geoid

Once the data have been stacked, the orbit error reduced and the spline adjustment done, all data points are supposed to reflect the MSS. We still have to subtract the SSDT to get the geoid. We used the Levitus (1982) model. Western boundary currents (e.g. the Gulf Stream) have dynamic topography of about one meter. Because of mismodeling errors in the Levitus model and of variability effects, a significant part of the signal may remain.

Prior to gridding and transforming into anomalies, we subtract a reference geoid computed from a global spherical harmonic model, to get a residual geoid. We used the OSU91A model (Rapp et al., 1991) which is complete to degree and order 360. The corresponding reference anomaly will be added back at the end of the process to the residual anomaly grid obtained by FFT. This is a usual remove-restore technique used to reduce effects of the flat Earth approximation and truncation errors when using FFT.

Fifth step: gridding

The gridding of the residual geoid heights is somewhat delicate because we have very good resolution along the tracks (1 point every 6 or 7 km) but relatively large gaps between different tracks, especially at latitudes smaller than 60°. After having tested different methods (average of nearest points with different kinds of weight, spline surface fitting) and different software, we selected a method which computes a spline surface with continuous curvature and eventually interior and boundary tension factors. The software, which is very fast, was taken from the GMT package (Smith & Wessel, 1990). For geoid gridding, it seems best to set the interior tension factor to zero. When dealing with an area with large data gaps (because of land or ice) and especially when located on the edges of the area, we empirically found that the residual geoid had to be constrained in these gaps by adding some points with zero value and eventually by using a tension factor along the edges. In high latitude areas close to the maximum latitude reached by the satellite, we discard the observations since inter-track geoid gradients (and therefore the gravity anomalies computed) are very sensitive to residual orbital errors for satellite tracks which are extremely close to each other - this not so much the case with the second method (see I.2).

Sixth step: FFT

We now have a regular grid in longitude and latitude, of residual geoid heights which we transform into residual gravity anomalies using the well-known FFT techniques (Schwarz et al., 1990) because its rapidity allows us to process large areas.

The sources of FFT errors that we have tried to reduce are the following:

a) Truncation errors: to minimize the truncation effects (due to the integration over a limited area) that appear on the edges of the area, we work, as said already, on residual grids

and we taper the edges of the grid by adding a tapered band all around the grid (for 5'x5' grids, a 1° wide band gave the best results). In addition, we work with areas bigger than the area (10° x 10°, practically) we are interested in, by 2 or 3 more degrees on each side of the area.

b) Flat Earth approximation: to perform FFT, the nodes should represent regularly spaced values. Of course a grid in longitude and latitude does not have the same horizontal scale at different latitudes. As a result, if we take into account the mean latitude to scale the horizontal grid step, the FFT will introduce errors except near the mean latitude. A first classical method to reduce these errors is to use a Lambert projection (for example) before doing the Fourier transform. But this is not easy when working on a large area; one would have to divide the area into different small regions, use several projections, and after transformation try to paste everything together. Another method was presented by Forsberg & Sideris (1993) and called «multi-band approach», which divides the area into narrow horizontal bands in which the horizontal grid step is quasi-constant. The successive overlapping bands are transformed seperately and then merged together, typically working on 3° wide bands. We adopted this method which is easy to use for large areas bounded by meridians and parallels.

c) Approximations in Stokes' integral: this approximation is often made when using Stokes' formula with FFT. Strang van Hees (1990), Forsberg & Sideris (1993) have shown that the Stokes integral can be well evaluated by a two dimensional convolution formula and transformed by FFT (instead of using only the leading term of the Stokes function as it is often done).

This improves the results, but even better seems to be the method of the gravity coating suggested by Farelly (1991).

To evaluate the errors due to the FFT, we made some tests over a 10°x10° area near Japan using the OSU91A geoid and gravity anomaly models from degree 180 to degree 360. This allowed us to compare the solutions obtained by FFT with an absolute reference, unfortunately looking only at wavelengths greater than 1°.

Table 1 summarizes the results of some tests we made to compare the different methods; the statistics are for a 7°x7° area (5'x5' grid) in the middle of the 10°x10° grid, to avoid edge effects. It is worth noting that this residual field ranges from -124 to +143 mGal.

Table 1. Comparison of three FFT methods when recovering the part of the OSU91A field above degree 180
(k is the wavenumber, S(ψ) the Stokes function, R the mean Earth radius)

Method	Kernel	Bands	RMS in mGal (min/max)
approximation of Stokes function	k	1 band (10°)	0.97 (-3.51/5.35)
		3° wide bands	0.47 (-1.02/2.51)
spherical FFT	$\frac{1}{FFT(S(\psi))}$	3° wide bands	0.45 (-0.86/1.68)
gravity coating method	$k-\frac{3}{2R}$	1 band	0.84 (-2.91/4.35)
		3° wide bands	0.35 (-0.59/1.54)

From these results we decided to choose the multi-band gravity coating method. In addition, we use a Wiener filter in the spectral domain as suggested by Forsberg & Solheim (1988), which has the following form when going from geoid heights to gravity anomalies:

$$W(k) = \frac{1}{1+ck^4} \qquad (1)$$

where c is set so that $W(k_r)=0.5$ when k_r is the wavenumber corresponding to the typical resolution expected from the data.

I.2- From deflection of the vertical to anomalies

The great advantage of this method is that it is only based on geoid gradients computed along the satellite profiles. So if there is locally a bias between two arcs, it has no effect on the results; all long wavelength errors have very small effects. As Sandwell (1992) showed it, the orbit error, which is mostly of long-wavelength nature, has a negligible effect, and no cross-over adjustment has to be done. To subtract the SSDT Levitus model, which is very smooth, is not necessary anymore, since its derivatives are several orders of magnitude smaller than the residual geoid gradients.

First step: data stacking

Stacking cycles together is still required because it diminishes noise and short wavelength phenomena of non geodetic origin that can appear on a cycle and not on others. So, as for the geoid, we worked with stacked data from ERMs.

Second step: north and east deflection computation

The along-track gradient (opposite of the deflection of the vertical) can be computed after fitting each arc with a smoothing spline. The question is how to obtain north and east gradients from gradients along up to six directions when dealing with three satellites, in benefitting from the maximum amount of information.

Sandwell (ibid.) has developped a method where north and east deflection grids are iteratively obtained from ascending and descending along-track deflection grids.

The method we present here is different and requires

cross-over location. The process is the following (fig. 3):

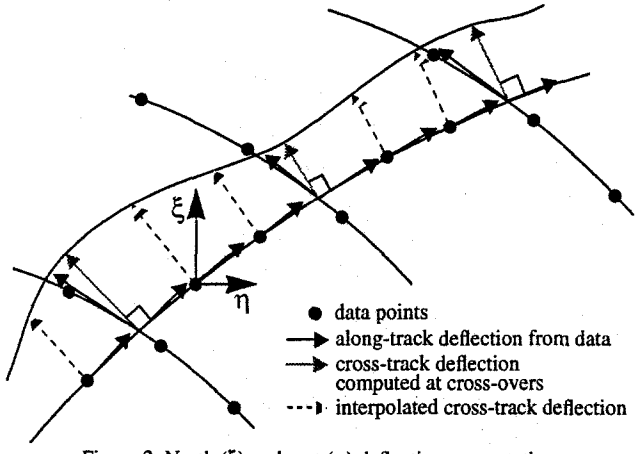

Figure 3. North (ξ) and east (η) deflection computation

- First we locate all cross-overs and interpolate the along-track deflection along each arc at the cross-overs, by deriving a smoothing spline that follows the profiles. Since these two components of the deflection will be used to compute cross-track deflection of both arcs, we only take cross-overs making a cross at significant angle, that is to say «UV» cross-overs, between a U arc and a V arc (if we call U arcs the ascending arcs of prograde satellites or the descending arcs of retrograde satellites, and V arcs the opposite). Taking «UU» or «VV» cross-overs would be dangerous since the azimuths of the arcs of such cross-overs are often close.

- Then we consider one arc after the other. We take an arc, compute the along-track deflection at each data point (again with smoothing splines). Then at each cross-over we compute the cross-track deflection from crossing along-track deflections computed at the first step. We interpolate these cross-track deflections at each data point with an Akima spline. Therefore we get along and cross-track deflections at each data point, and from these two components we recover north (ξ) and east (η) deflections.

Regarding the cross-track deflection interpolation: at the extremity of an arc, after the last cross-over, the cross-track deflection at this last cross-over is extrapolated to the end of the arc. Every data point which is too far from the nearest cross-over of its arc is eliminated. The maximum distance for interpolation or extrapolation has been set to 15 km for dense data (Geosat GM) and 60 km for merged ERMs of Geosat, ERS-1 and Topex-Poseidon.

Third step: removal of reference model

We subtract the spherical harmonic reference model from north and east deflections.

Fourth step: gridding

We have north and east residual deflections at data points. The gridding of these values is performed with the same method and software used in the case of the geoid.

Fifth step: FFT

We use the following formula, with approximation of the Stokes function by the leading term:

$$\tilde{\Delta g}(k) = \frac{i\gamma}{k} \cdot W(k) \cdot \left[k_x \tilde{\eta}(k) + k_y \tilde{\xi}(k)\right] \qquad (2)$$

where:

$$k = \sqrt{k_x^2 + k_y^2}$$

k_x and k_y being the wavenumbers in west-east and south-north directions, respectively.

To try to minimize the errors due to the flat Earth approximation, we again work on narrow horizontal bands, on the principle suggested by Forsberg & Sideris (ibid.). We also apply a Wiener filter in the frequency domain, which is in that case:

$$W(k) = \frac{1}{1 + dk^2} \qquad (3)$$

Finally, we obtain a residual FAA grid, which is added to the reference model to get the final grid.

II- RESULTS AND COMPARISONS

II.1- Working with Geosat, ERS-1 and Topex-Poseidon ERMs

The first computation is done with non-dense data sets. R.H. Rapp provided a one year stacked data set of Geosat ERM (November 1986 to October 1987, Wang & Rapp, 1992). ERS-1 IGDRs with improved orbit were provided by C.C. Tscherning and were stacked over a year (14th April 1992 to 4th May 1993). Topex-Poseidon data were stacked at GRGS, again over one year (13th October 1992 to 14th October 1993).

The studied area goes from 25°W to 60°E and from 30°N to 82°N. We work on 5'x5' grids.

Geoid precision

For the geoid computation, Topex-Poseidon was first adjusted over the whole globe as explained before, the RMS at cross-overs going from 3.4 cm before adjustment to 1.9 cm after. Then ERS-1 and Geosat were adjusted on Topex-Poseidon, over a large area (70°W to 120°E and 10°S to 82°N) containing the region of interest, to be sure that all arcs are well constrained, especially ERS-1 northern arcs (as checked with our visualization software). The RMS at cross-overs after adjustment were the following:

Geosat/Geosat :	10.6 cm
ERS-1/ERS-1 :	6.5 cm
Topex/Topex :	1.9 cm
Topex/Geosat :	6.8 cm
Topex/ERS-1 :	6.2 cm
Geosat/ERS-1 :	8.8 cm
All cross-overs :	7.8 cm

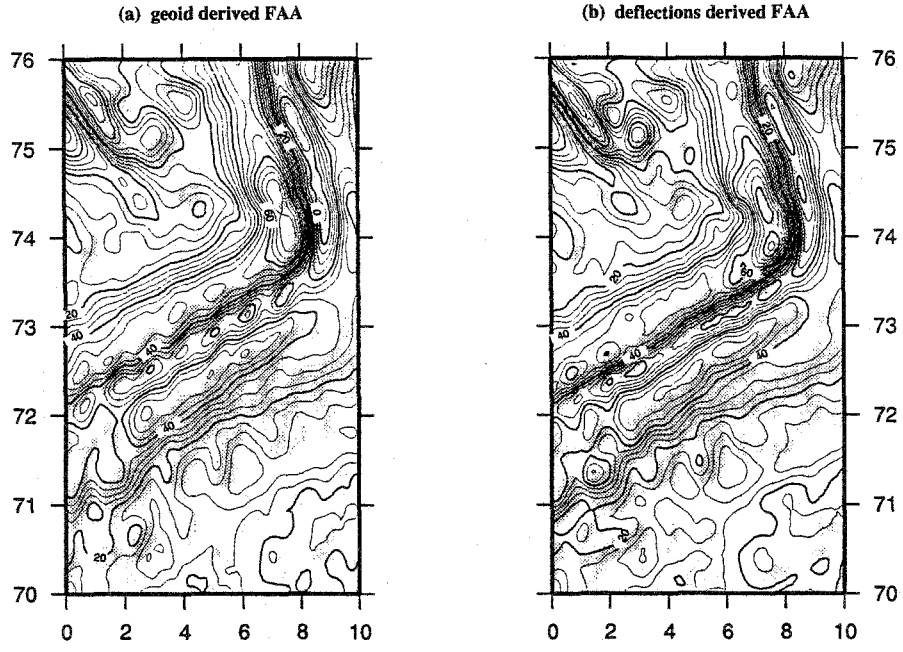

figure 4: Comparison between geoid and deflection derived grids (contour every 5 mGal)

As said before, after spline adjustment all cross-over differences were nullified. So we may say that the precision of our MSS is about 8 cm where we have data.

It is difficult to give a long wavelength precision to our geoid, but here are some figures to give an idea: Levitus SSDT surface precision in Northern Atlantic Ocean is said to be around 10 cm for long wavelengths. The effects of currents that have a period longer than a year are believed to be a few centimeters in this region, except for the Gulf Stream of which the position changes.

The short wavelength precision is limited by the poor inter-track resolution, especially at low latitudes. At 30° in latitude, we find some geographical points in the grid which are 35 km away from the nearest data point. The short wavelength information cannot be invented in places where we have no data. To quantify its importance, we high-pass filtered a high resolution geoid which we computed with Geosat dense data (described in part III) over the Mid-Atlantic Ridge, where we find very large high frequency signal. After high-pass filtering, keeping wavelengths under 35 km and rejecting those above 40 km, the residual high frequencies went up to 20 cm, with an RMS of 2.5 cm. Of course the precision of recovery of these terms increases with latitude.

Computation of FAA grids

The geoid derived anomaly grid was obtained by FFT as described before; north and east deflections were gridded and also converted into anomalies. Both conversions included a Wiener (low-pass) filter with a half-cut at 35 km.

Comparison

The two grids show no difference at wavelengths greater than 100 km. The RMS differences that we observed between the two grids are 3.5 mGal in an area around 70°N, and 6.7 mGal in an area around 40°N.

When looking at the maps (fig. 4), there are two points to note: first, the geoid method sometimes generates lineaments that can be seen on the maps using a shading graphic technique; the deflection method gets rid of these effects. The second point is that the deflection method provides more continuity in the short wavelength features. This can be seen on the figure.

We performed some comparisons with marine cruises, in different areas. The geoid and the deflection methods lead to quite similar results in places where the cross-over discrepancies are small, but the difference can be appreciable in other places, as shown from comparison with cruise data, e.g. one (Sharman and Metzger, 1994) located around 15°W-55°N (see table 2). The external grid is from Sandwell & Smith (ibid.). Figure 5 shows the correlation between the cruise data and the deflections derived FAA grid interpolated along the cruise, after a -14 mGal bias adjustment of the cruise, probably due to a reference system error (the bias is practically equal to the Postdam correction).

Table 2.
Comparison with marine data in the case of non-dense altimetric data

Grid compared	linear correlation with cruises	std deviation of difference	mean difference
Geoid method	0.929	9.42 mGal	-14.2 mGal
Deflection method	0.957	7.75 mGal	-13.7 mGal
External grid	0.921	10.44 mGal	-13.05 mGal

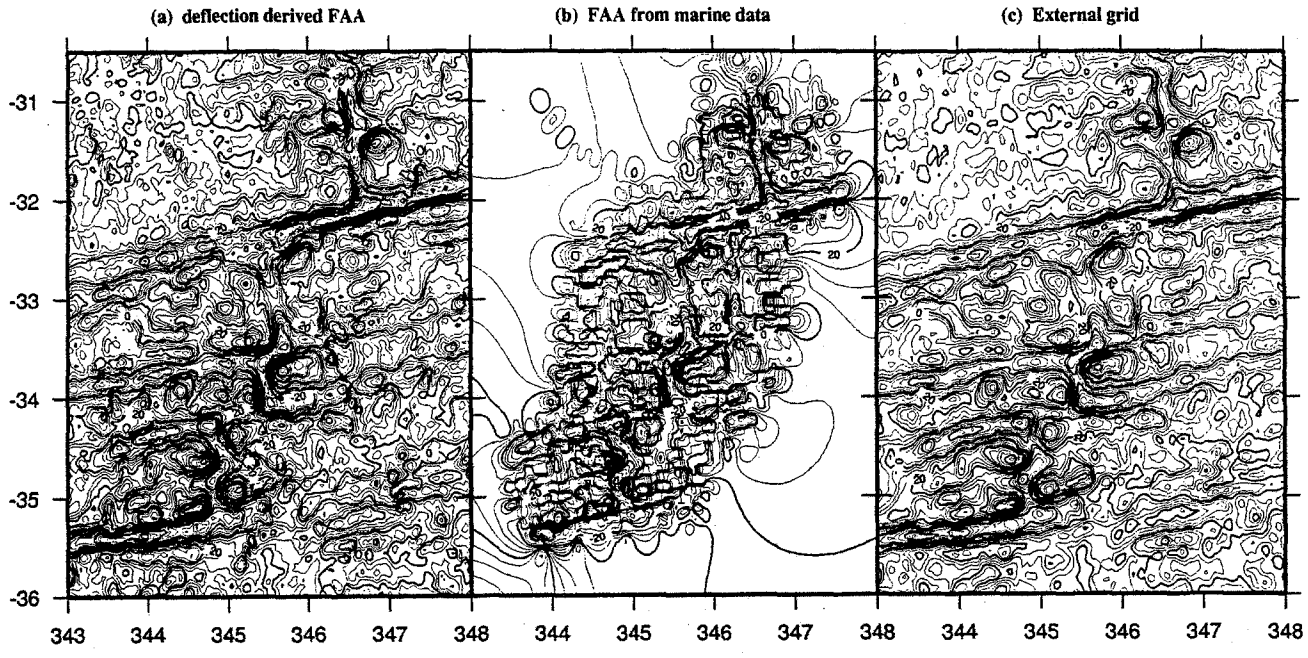

figure 6: Comparison of FAA grids over the Mid Atlantic Ridge (contour every 5 mGal)

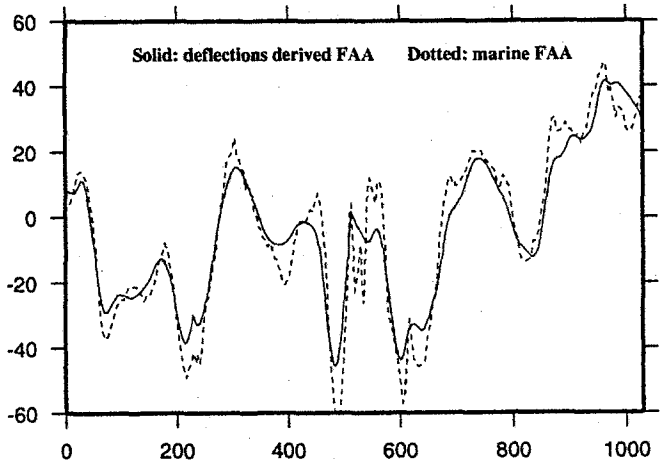

Figure 5: Correlation of the deflection derived grid with a Geodas marine cruise (units: km and mGal)

In that first situation (non-dense data), the deflection method appears to be superior to the geoid method, but the geoid method does not give bad results and has the advantage of providing, as intermediate product, a geoid grid which can be used for other purposes.

II.2- Working with Topex-Poseidon and Geosat GM

This second determination is made along the Mid-Atlantic Ridge, from 20°W to 9°W and from 38°S to 30°S, with 2'x2' grids by Neumann (1993), covering the area chosen, for the sake of comparison (fig. 6).

When using the geoid method, the Geosat GM tracks are so close to each other that a simple error of 2 cm between two parallel arcs separated by 2 km creates a geoid gradient which produces a gravity anomaly error of about 10 mGal. As a result, the geoid derived FAA grids are so marked by the satellite tracks that it hides the short wavelength signal (fig. 7a shows these residuals level problems in the geoi grid). It is clear that our geoid method, despite the efforts we have made to bring it to an otherwise satisfactory level, fails in the case of dense data.

On the other hand, the deflection derived map shows very clear details. We compared our grid and an external grid (Sandwell & Smith, ibid.) to marine data (Marathon 10 and Plume 4 & 5 validated and adjusted cruises, Neumann et al., 1993) which are considered as a very good reference (internal standard deviation at cross-overs was reported to be less than 4 mGal). The grids can be seen in figure 6. The quality of the results is shown by numerical comparison with the marine cruises (table 3). The comparison is made between marine data points and values interpolated from the altimetry derived grids.

Table 3.
Comparison with marine data in the case of dense altimetric data

Grid compared	linear correlation with cruises	std deviation of difference	mean difference
BGI grid	0.963	7.0 mGal	0.3 mGal
External grid	0.959	8.3 mGal	1.8 mGal

Nota: our deflection method requires cross-over location, which we consider is no major handicap with today's machines. It is even feasible with a modest workstation: we produced a FAA grid using Geosat GM data over a large region (57°W to 183°W and 53°S to 30°S) containing 1.500.000 cross-overs. It took 3.5 days from beginning to end with a Sun Sparc station IPX.

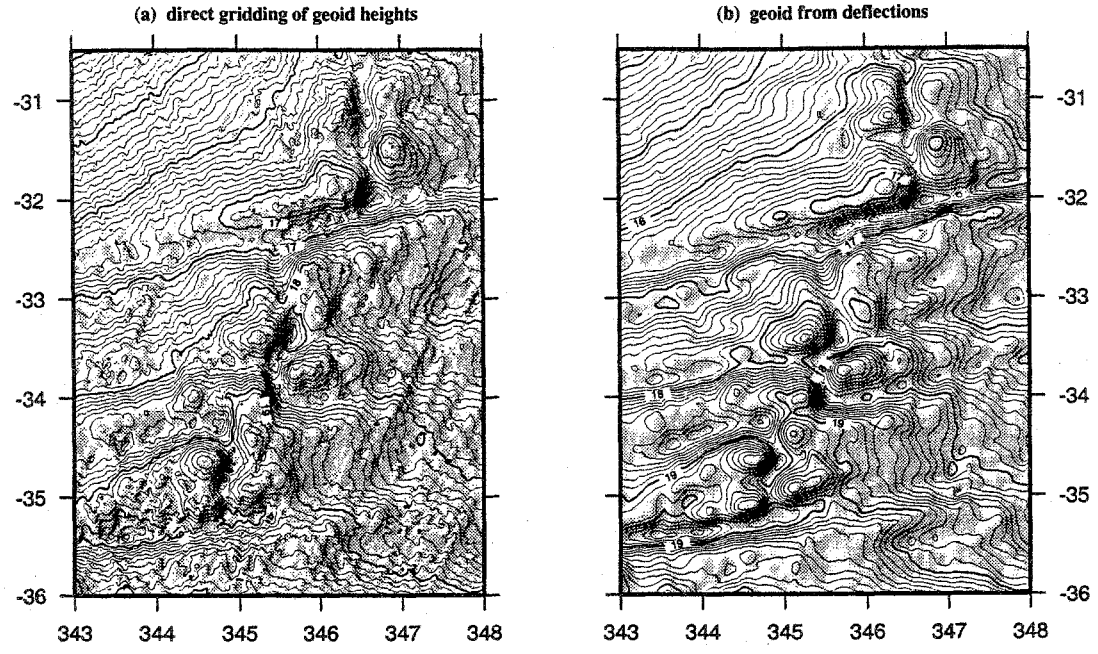

figure 7. Geoid grids with 10 cm coutour

III- COMPUTATION OF A GEOID GRID WITH DENSE DATA

The difference between the poor looking geoid derived FAA grid and the deflection derived grid lead us to try to compute the geoid from deflections of the vertical using FFT.

We have:

$$\begin{cases} \tilde{\xi}(k) = -ik_y\tilde{N}(k) \\ \tilde{\eta}(k) = -ik_x\tilde{N}(k) \end{cases} \quad (4)$$

Thus:

$$k_y\tilde{\xi}(k) + k_x\tilde{\eta}(k) = -ik^2\tilde{N}(k) \quad (5)$$

Consequently:

$$\tilde{N}(k) = \frac{i}{k^2}\cdot\left[k_y\tilde{\xi}(k) + k_x\tilde{\eta}(k)\right] \quad (6)$$

Using the usual remove-restore technique and again the multi-band approach, we computed the geoid surface shown in figure 7b. The comparison between this surface and the Topex-Poseidon profiles shows a RMS difference of 10 cm. Compared to the quality of the Topex-Poseidon data, this might be explained by the larger errors in the Geosat data which are simultaneously used, also by the sea surface topography model used..

Besides this approach, and of course least squares collocation, there are other ways to compute a geoid from geoid slopes (Sandwell, 1987) but we did not try any at the moment.

CONCLUSION

In this paper, two methods to convert satellite altimetry data into free air gravity anomalies have been presented with an emphasis on practical aspects.

A geoid was computed with stacked ERMs of Geosat, ERS-1 and Topex-Poseidon over an area going from 25°W to 60°E and from 30°N to 82°N, following an orbit error adjustment and a «spline adjustment» which avoids or at least diminishes artefacts due to remaining cross-over errors.

A new algorithm for gridding north and east deflections of the vertical was presented.

The conversion of the geoid grid and of the deflection grids into FAA has been done with FFT techniques, taking special care of the different errors induced by these techniques: the truncation error, the flat Earth approximation and the approximation of the Stokes integral. A Wiener filter was applied in the spectral domain.

Unlike collocation or similar statistical estimation methods, the FFT approach does not provide the error estimate of the predicted anomalies. Their accuracy can be evaluated only with recourse to external data checks.

The comparison with marine gravity data allows us to say that both methods, via geoid and via deflections, lead us to satisfactory results when working with these ERMs, altough the poor inter-track spacing doesn't allow a high resolution product. The results are quite similar in areas of low variability and medium frequency signal, but the deflection method appears to be superior in other areas, giving no artificial lineaments along sub-satellite tracks and more continuous features.

When working with dense data, i.e. Geosat GM south of

30°S, the geoid method is not workable anymore, because the very small inter-track spacing creates high cross-track geoid gradients when gridding the geoid. But the deflection method leads to better FAA maps. Over the Mid Atlantic Ridge, where important high frequency signal is present, our map differs from dense marine cruises by 7.0 mGal RMS, which appears to be slightly better than the results obtained by Sandwell & Smith with a different algorithm.

A high resolution geoid was computed from the north and east deflection grids via FFT, not showing the lineaments that were present on the grid directly obtained from geoid heights.

The deflection of the vertical method, after that empirical comparison, appears to be a good method to use to compute FAA from altimetry data. The ERS-1 170 day orbit mission, hopefully followed by a slightly shifted mission with the same inter-track spacing, ground segment operations permitting, promises fairly dense data of very good quality, allowing the production of global high resolution maps of geoid and FAA.

Acknowledgements

We thank R.H. Rapp for providing Geosat one year mean sea surface height track, C.C. Tscherning for providing ERS-1 data, C. Brossier for providing the Topex mean arc and G. A. Neumann for providing Marathon 10 and Plume 4 & 5 validated and adjusted cruises, as well as the corresponding FAA grid (Neumann et al., ibid.).

References

Akima, H. (1970) A new method of interpolation and smooth curve fitting based on local procedures, J. of the Assoc.for Computing Machinery, Vol.17, No.4, pp.589-602.

Balmino, G. (1992) Orbit choice and the theory of radial orbit error for altimetry, in Satellite Altimetry in Geodesy and Oceanography, R. Rummel and F. Sanso (Eds), Springer-Verlag, 243-315.

Farelly, B. (1991) The geodetic approximations in the conversion of geoid height to gravity anomaly by Fourier transform, Bull. Géodésique, 65:92-101.

Forsberg, R. and D. Solheim (1988) Performance of FFT methods in local gravity field modelling, Chapman Conference on progress in the determination of the Earth's gravity field, pp. 100-103.

Forsberg, R. and M.G. Sideris (1993) Geoid computations by the multi-band spherical FFT approach, Manuscripta Geodaetica, Vol. 18, No. 2, pp. 82-90.

Haxby, W.F., Karner G.D., Labrecque J.L. and Weissel J.K. (1983) Digital images of combined oceanic and continental data sets and their use in tectonic studies. EOS Trans. Am. geophys. Un., 64, pp. 995-1004.

Knudsen, P., O.B. Andersen and C.C. Tscherning (1992) Altimetric gravity anomalies in the Norwegian-Greenland Sea - Preliminary results from the ERS-1 35 days repeat mission, Geophys. Res. Lett., Vol. 19, No. 17, pp. 1795-1798.

Levitus, S. (1982) Climatological Atlas of the World Ocean NOAA, Geophysical Fluid Dynamics Laboratory, Professional Paper 13, Rockville, MD.

Neumann, G.A., D.W. Forsyth and D.T. Sandwell (1993) Comparison of marine gravity from shipboard and high-density satellite altimetry along the Mid-Atlantic Ridge, Geophys. Res. Lett., Vol. 20, No. 15, pp. 1639-1642.

Rapp, R.H. and T. Basic (1992) Oceanwide gravity anomalies from Geos-3, Seasat and Geosat altimeter data, Geophys. Res. Lett., Vol. 19, No. 19, pp. 1979-1982.

Rapp, R.H., Y.M. Wang and N.K. Pavlis (1991) The Ohio State 1991 geopotential and sea surface topography harmonic coefficient models, Rep. 410, Dep. of Geod. Sci. and Surv., The Ohio State Univ., Columbus.

Sandwell, D.T. (1987) Biharmonic spline interpolation of Geos-3 and Seasat altimeter data, Geophys. Res.Lett., Vol. 14, No. 2, pp. 139-142.

Sandwell, D.T. (1992) Antartic marine gravity field from high-density satellite altimetry, Geophys. J. Int. 109, 437-448.

Sandwell, D.T. and W.H.F. Smith (1992) Global marine gravity from ERS-1, Geosat and Seasat reveals new tectonic fabric, AGU Fall meeting, G42D-7.

Schwarz, K.P., M.G. Sideris and R. Forsberg (1990) The use of FFT techniques in physical geodesy, Geophys. J. Int 100, 485-514.

Sharman, G.F. and D. Metzger (1994) National Geophysical Data Center's GEODAS CD-ROM Project, submitted to Bulletin d'information, Bureau Gravimétrique International.

Smith, W.H.F. and P. Wessel (1990) Gridding with continuous curvature splines in tension, Geophysics, Vol. 55, pp. 293-305.

Strang van Hees, G. (1990) Stokes formula using Fast Fourier Techniques, Manuscripta Geodaetica, Vol. 15, pp. 235-239.

Wang, Y.M. and R.H. Rapp (1992) The determination of a one year mean sea surface height track from Geosat altimeter data and ocean variability implications, Bull. Géodésique, 66:336-345.